

**Coherent control in the classical limit: Symmetry breaking in an optical lattice**Michael Spanner,<sup>\*</sup> Ignacio Franco,<sup>†</sup> and Paul Brumer*Chemical Physics Theory Group, Department of Chemistry, and Center for Quantum Information and Quantum Control, University of Toronto, Toronto, Ontario, Canada M5S 3H6*

(Received 23 June 2009; revised manuscript received 31 August 2009; published 3 November 2009)

The quantum-to-classical transition of a symmetry-breaking coherent control scenario is computationally demonstrated in an optical lattice arrangement. Control is shown to survive in the classical limit and, for small effective  $\hbar$ , to be comparable in magnitude to quantum control. Moderate decoherence is seen to eliminate structure from the momentum space distribution, but not to cause loss of control. The proposed scenario is designed so as to be demonstrable experimentally in a moving or shaken one-dimensional optical lattice.

DOI: [10.1103/PhysRevA.80.053402](https://doi.org/10.1103/PhysRevA.80.053402)

PACS number(s): 32.80.Qk

**I. INTRODUCTION**

Coherent control of molecular processes arises from the interference between multiple pathways to the same final state [1,2], typically induced via laser irradiation. Recently, theoretical studies have shown that analogous processes can arise in certain scenarios in classical mechanics [3,4] and that such control can persist in the classical limit [5]. Considerations based on nonlinear response and on interference viewed via the Heisenberg representation [6,7] show that when control survives in the classical limit it does so because the interference terms contributing to the quantum dynamics are externally driven, i.e., proportional to the amplitude of the external laser fields. In this sense, the quantum interference contributions differ qualitatively from those in, for example, the double slit experiment.

The possibility of a nonzero classical limit to the quantum interference phenomena responsible for quantum control is significant and in need of careful exploration. In this paper, we computationally examine the approach to the classical control limit in a proposed optical lattice scenario expected to be doable experimentally. The design allows one to explore both control as an effective  $\hbar \rightarrow 0$  as well as the comparative effect of decoherence on quantum control. The computational results below also emphasize differences in quantum response in the domain of classically regular vs chaotic dynamics.

As a particular control scenario, we focus on symmetry breaking in which a spatially symmetric system is irradiated with a laser field with frequency components  $\omega$  and  $2\omega$ . Such fields generate phase-controllable net dipoles or currents without introducing a bias in the potential (see, e.g., Refs. [1,3,5,8–10]). Our proposed system is a moving or shaken one-dimensional optical lattice [11,12], which (as shown below), through a gauge transformation, can be viewed as a stationary spatially symmetric periodic potential interacting with a space homogeneous electric field. We consider both the  $\hbar \rightarrow 0$  limit as well as the effect of decoherence, the latter

by adding controlled amounts of decoherence through random momentum jumps induced by spontaneous emission. This allows an exploration of the effect of decoherence on a control scenario that can persist in the classical limit and, hence, in which matter interference plays a different role than traditionally envisioned.

Recently, experiments on Bose-Einstein condensates (BEC) in shaken optical lattices demonstrated a reversible superfluid-Mott insulator phase transition by changing the strength of the driving [13]. Although we do not require coherent multiparticle effects present in BECs, the coherent initial state provided by BECs would be necessary for experimental observation of the quantum-classical transition discussed below.

In this paper below, Sec. II introduces the details of the shaken optical lattice and discusses its relationship to the traditional dipole-field interaction scenario. Section III provides numerical results, showing details of the control in the quantum regime, and its approach to the classical limit. The significance of these results to an understanding of coherent control is discussed in the summary provided in Sec. IV.

**II. FORMAL CONSIDERATIONS****A. Physical system**

Consider an atom interacting with a longitudinally shaken one-dimensional optical lattice. The associated Hamiltonian is

$$H = \frac{P^2}{2m} + U f_1(t) \cos[2kx - \beta f_2(t)], \quad (1)$$

where  $P$  is the atom momentum and  $m$  is its mass. The term  $U$  is the well depth created by the optical lattice with wave vector  $k$ . For an off-resonant interaction  $U = \alpha I_0/4$  for where  $\alpha$  is the atomic polarizability and  $I_0$  is the peak lattice intensity. The pulse shapes  $f_1(t)$  and  $f_2(t)$  describe the temporal envelope and spatial shaking motion of the lattice, respectively, with  $\beta$  controlling the strength of the shaking. Such spatial motion of the lattice is experimentally achieved by applying a phase modulation to one of the counterpropagating beams that generate the optical potential [11]. Below we consider two-frequency driving fields with frequencies  $\omega$  and  $2\omega$ ,

<sup>\*</sup>Present address: Steacie Institute for Molecular Sciences, National Research Council of Canada, Ottawa, ON, Canada K1A 0R6.

<sup>†</sup>Present address: Department of Chemistry, Northwestern University, Evanston, Illinois 60208-3113.

$$f_2(t) = \cos(\omega t + \phi_{\text{rel}}) + s \cos(2\omega t), \quad (2)$$

where  $s$  controls the ratio of field amplitudes ( $s=1$  in all calculations below) and  $\phi_{\text{rel}}$  is the relative phase between the driving fields. The atomic wave function  $\Psi(x, t)$  satisfies the Schrödinger equation  $i\hbar \partial \Psi(x, t) / \partial t = H(t) \Psi(x, t)$ . Some features of the quantum dynamics of this system have been reported previously [14].

### B. Reduced units and effective $\hbar$

For the purpose of investigating the classical limit, we would like to take  $\hbar \rightarrow 0$ . Although  $\hbar$  is a fixed constant in nature, an effective Planck's constant, which can be varied by changing the lattice parameters, can be defined by casting the problem in reduced units. For instance, by rescaling the coordinates as

$$\theta = 2kx, \quad (3a)$$

$$P_\theta = P(2k/\omega m), \quad (3b)$$

$$\tau = \omega t, \quad (3c)$$

and defining

$$\mathcal{U} = (2k/\omega)^2 (U/m), \quad (4)$$

the Hamiltonian becomes

$$\mathcal{H} = \frac{P_\theta^2}{2} + \mathcal{U} f_1(\tau) \cos[\theta - \beta f_2(\tau)], \quad (5)$$

where  $\mathcal{H} = (2k/\omega)^2 H/m$ . The classical equations of motion are then

$$\dot{\theta} = \frac{\partial \mathcal{H}}{\partial P_\theta} = P_\theta, \quad (6a)$$

$$\dot{P}_\theta = -\frac{\partial \mathcal{H}}{\partial \theta} = \mathcal{U} f_1(\tau) \sin[\theta - \beta f_2(\tau)]. \quad (6b)$$

Note that, apart from the pulse shapes  $f_1(\tau)$  and  $f_2(\tau)$ , the classical dynamics is governed by two remaining free parameters  $\beta$  and  $\mathcal{U}$ .

The associated quantum-mechanical equations allow for the introduction of an effective Planck's constant  $\hbar_e$ . Specifically, in the reduced units the Schrödinger equation becomes

$$i\hbar_e \frac{\partial \Psi(\theta, \tau)}{\partial \tau} = \left\{ -\frac{\hbar_e^2}{2} \frac{\partial^2}{\partial \theta^2} + \mathcal{U} f_1(\tau) \cos[\theta - \beta f_2(\tau)] \right\} \Psi(\theta, \tau), \quad (7)$$

where

$$\hbar_e = \hbar(2k)^2/(\omega m) \quad (8)$$

is the effective  $\hbar$  in the reduced units. The term  $\hbar_e$  can be tuned independently of  $\mathcal{U}$  and  $\beta$  by varying the lattice parameters  $k$  and  $\omega$ . Hence, the  $\hbar_e \rightarrow 0$  limit can, in principle, be accessed experimentally. Analogous experimental control over the effective Planck's constant has been previously re-

ported [15] in the context of cold cesium atoms in an amplitude-modulated standing wave of light.

### C. Equivalence with dipole driving

This setup is related to a traditional coherent control scenario with dipole interaction  $\mu E_0(t)$  through a gauge transformation. Specifically, consider a moving reference frame defined by the coordinate transformation

$$z = \theta - \beta f_2(\tau) \quad (9)$$

and employ the gauge transformation

$$\Psi'(z, \tau) = e^{izA(\tau)/\hbar_e} \Psi(z, \tau), \quad (10)$$

where

$$A(\tau) = -\beta \dot{f}_2(\tau). \quad (11)$$

The Schrödinger equation takes the form  $i\hbar_e \partial_\tau \Psi'(z, \tau) = \mathcal{H}'(\tau) \Psi'(z, \tau)$ , where

$$\mathcal{H}'(\tau) = \frac{P_z^2}{2} + \mathcal{U} f_1(\tau) \cos(z) + zE(\tau), \quad (12)$$

$P_z = \dot{z} + \beta \dot{f}_2(\tau)$  is the momentum conjugate to  $z$ , and

$$E(\tau) = \beta \ddot{f}_2(\tau). \quad (13)$$

Hence, the optical lattice scenario is directly related to the traditional control scenario; the system represents either an atom in a shaking optical lattice ( $\mathcal{H}$  gauge) or a charged atom in a static and spatially symmetrical optical lattice that is driven by an oscillating electric field  $E(\tau)$  ( $\mathcal{H}'$  gauge). All numerical calculations presented below refer to the  $\mathcal{H}$  gauge as this is the scenario more easily accessible to optical lattice experiments. In the results reported below, the final distributions of the photoinduced momentum are taken after the field  $f_2(\tau)$  is turned off. In this regime, the momentum in both gauges coincides.

### D. Decoherence

In addition to the  $\hbar_e$  dependence of the isolated system dynamics, we also consider the effect of decoherence. Decoherence associated with the loss of quantum information of the system due to interaction with the environment is a phenomenon often invoked as the cause of loss of quantum control. In order to study the effects of decoherence in an experimentally accessible way, we include spontaneous emission (scattering) into our model. We use a simple model of spontaneous emission, previously used for studies of decoherence in optical lattice implementations of the delta kicked rotors [16]. This model introduces random momentum jumps, on the order of the lattice photon momentum, into the wave-function dynamics. The probability of a jump occurring is uniformly distributed in time. The dynamics with decoherence is calculated using a Monte Carlo wave-function method: the Schrödinger equation (7) is solved many times for different realizations of the random momentum shifts, and all observables are averaged over these different realizations. Although spontaneous emission is a quan-

tum effect, the present model consisting of random momentum recoils can be easily applied to the classical models. Experimentally, the rate of spontaneous emission, and hence the rate of the momentum jumps, can be controlled by tuning the optical lattice closer or farther from an atomic resonance. Alternatively, an additional laser field can be added, whose sole purpose is to couple the system to a separate decaying level [17].

Note that this implementation of decoherence through noise requires averaging over an ensemble of realizations each one evolving unitarily. The corresponding ensemble of unitary evolutions represents a nonunitary evolution of the density matrix of the system. By contrast, “true” decoherence occurs for a *single*-quantum system that becomes entangled with environmental degrees of freedom. The unitary deterministic evolution of the system plus environment leads to a nonunitary evolution of the reduced density matrix of the system. This conceptual difference between noise and true decoherence is known [18,19]. However, unless this difference is probed explicitly, the noise model is expected to mimic very well the effects of decoherence since they both effectively lead to a damping of spatial coherences that causes interference patterns to decay [18], which is the effect that we are interested in here.

### III. COMPUTATIONAL RESULTS

#### A. Simulation parameters

In order to computationally explore the control dynamics, we need to select a specific pulse shape and specify the initial conditions. The envelope  $f_1(\tau)$  is chosen to be

$$f_1(\tau) = \sin^2\left(\frac{\pi\tau}{2\sigma_\tau}\right), \quad (14)$$

where  $\sigma_\tau=100$  is the full width at half maximum of the pulse, and the total pulse duration is  $2\sigma_\tau$ . In addition to this specific pulse shape, we introduce an “absolute” phase  $\phi_{\text{abs}}$  of the shaking motion of the lattice

$$\mathcal{H} = \frac{p_\theta^2}{2} + \mathcal{U}f_1(\tau)\cos[\theta - \beta f_2(\tau + \phi_{\text{abs}})], \quad (15)$$

where  $\phi_{\text{abs}}$  determines the temporal shift between the envelope  $f_1(\tau)$  and the underlying oscillations  $f_2(\tau)$ . Computations below assume  $\mathcal{U}=0.1$  and  $\beta=1$ .

Classical and quantum results are compared below. In doing so, all classical and quantum initial conditions are related by

$$\Psi_0(\theta) = \sqrt{\mathcal{D}_c(\theta)}, \quad (16)$$

where  $\Psi_0(\theta)$  is the initial quantum wave function,  $\mathcal{D}_c(\theta)$  is the distribution of initial classical trajectory positions, which all have zero initial momentum  $P_\theta=0$ . With this definition  $|\Psi_0(\theta)|^2=\mathcal{D}_c(\theta)$ , i.e., the initial quantum and classical spatial probability distributions are the same. The initial quantum states are chosen to be real and hence have zero initial momentum in the semiclassical sense  $|\Psi_0(\theta)|e^{ip(x)x}$ , where  $p(x)=0$ .

The classical dynamics of this system exhibits interesting structure, motivating a detailed examination of several different initial states. Specifically, the classical system displays chaotic dynamics for some regions of the initial phase space. These chaotic regions lie on the crests of the optical lattice and correspond to bifurcation instabilities (i.e., small perturbations cause rapid oscillations between falling off the crest to the left or right). This suggests an examination of the quantum/classical transition for regular and chaotic regions of the phase space. To this end, we examine three initial states: a spatially uniform state with

$$\mathcal{D}_c^{(u)}(\theta) = 1/(2\pi) \quad (17)$$

and two additional initial states localized in the regular  $\mathcal{D}_c^{(r)}(\theta)$  and chaotic  $\mathcal{D}_c^{(c)}(\theta)$  regions, respectively,

$$\mathcal{D}_c^{(r)}(\theta) = \eta^{(r)} \exp[-7(\theta - \pi)^2],$$

$$\mathcal{D}_c^{(c)}(\theta) = \eta^{(c)} \exp[-7\theta^2],$$

where  $\eta^{(r)}$  and  $\eta^{(c)}$  are the appropriate normalization factors for the distributions. Note that although the initial quantum state still has zero semiclassical (and average) momentum, the presence of spatial localization implies nonzero momentum in the quantum case through the uncertainty principle  $\Delta\theta\Delta P_\theta \sim \hbar_e$ . Thus, some dynamical differences arising from differences in the initial state are expected in the latter two cases in the large  $\hbar_e$  limit.

#### B. Classical dynamics

Consider first control in the classical system. Results are shown in the first column of Fig. 1, which shows the final average momentum  $P_{\theta,\text{avg}}$  (averaged over all initial trajectories) as a function of  $\phi_{\text{rel}}$  and  $\phi_{\text{abs}}$ . The top row presents results for the uniform distribution, while the middle and bottom plots correspond to the regular and chaotic distributions, respectively. The color scale used for all control maps is shown in the bottom right of Fig. 1. Note that all plots shown in the figure are normalized to their individual maximum values. For the quantitative measure of the range of control, see Fig. 2 discussed below.

In all cases, regions of control, where nonzero average momentum has been imparted to the atoms, are seen. This nonzero momentum can be either positive (right moving atoms) or negative (left-moving atoms), depending on the particular choice of phases of the driving lattice. The classical control displays a strong  $\phi_{\text{rel}}$  dependence, showing that this traditional coherent control strategy (i.e., the dependence of the outcome of a driven process on the relative phase of two driving frequencies) survives in classical mechanics. Note that for regular dynamics, the results are independent of  $\phi_{\text{abs}}$ , whereas the chaotic regions show a strong  $\phi_{\text{abs}}$  dependence. Hence, the  $\phi_{\text{abs}}$  dependence seen for the uniform initial distribution originates from the chaotic regions. Such  $\phi_{\text{abs}}$  dependence arises in the chaotic dynamics since changing  $\phi_{\text{abs}}$  one is changing the relative delay between the pulse envelope and the underlying oscillations; thus one perturbs slightly the peak force attained in each cycle of the driving

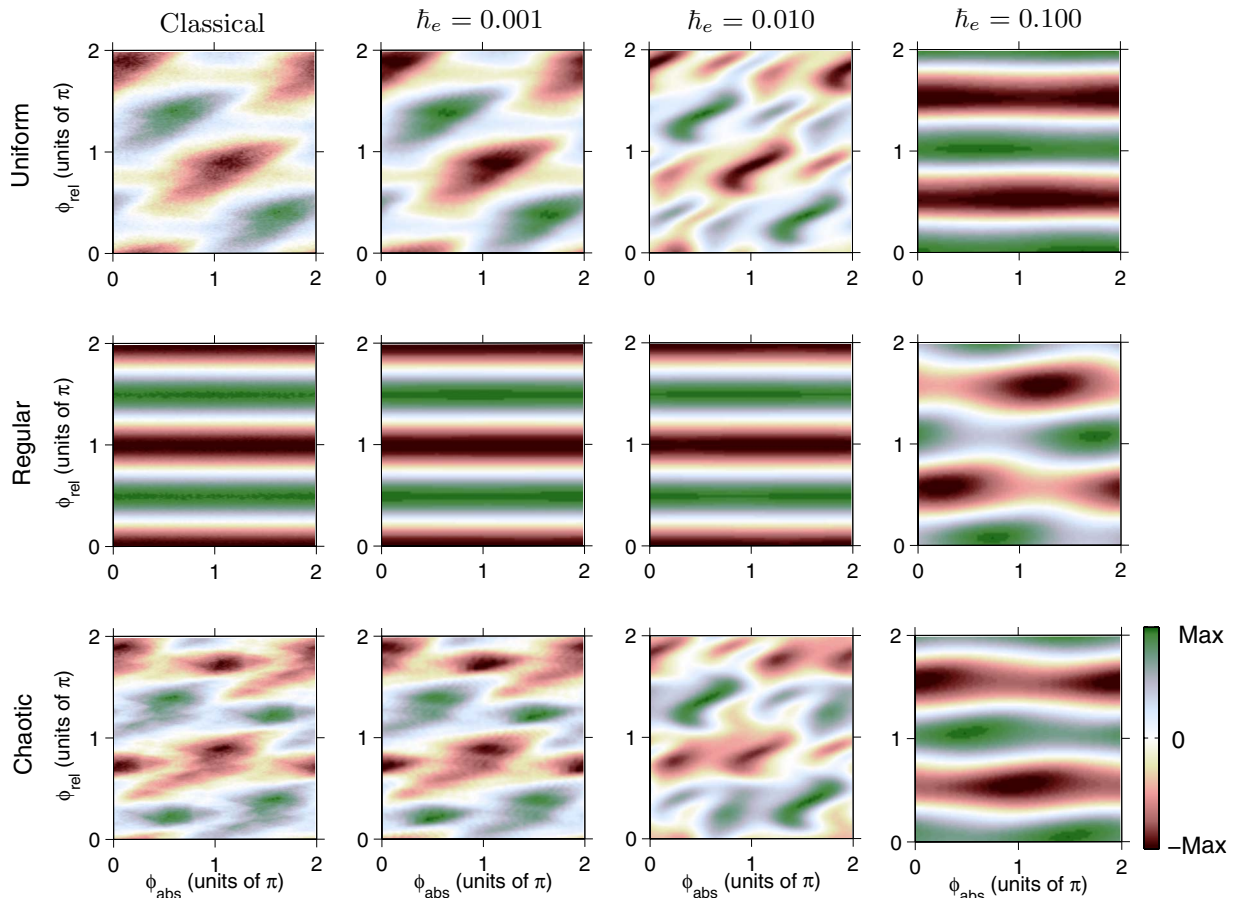


FIG. 1. (Color online) Control dynamics. Final average momentum for the classical and quantum systems. The top row is for the uniform initial state, while the middle and bottom rows correspond to the regular and chaotic initial state. The first column plots the classical results, while the remaining columns plot the quantum results for three values of  $\hbar_e=0.001, 0.01$ , and  $0.1$ .

field. Since chaotic dynamics is extremely sensitive to small perturbations, a strong  $\phi_{\text{abs}}$  dependence results.

### C. Quantum-classical correspondence in the $\hbar_e \rightarrow 0$ limit

Of particular interest is the quantum control dynamics as  $\hbar_e \rightarrow 0$ . This is shown in Fig. 1 for three values of  $\hbar_e$  (0.1, 0.01, and 0.001) for the three initial states considered. Plotted is the expectation value  $\langle P_\theta \rangle$  of the final momentum distribution as the control measure, i.e., the quantum analog of  $P_{\theta,\text{avg}}$ .

Several points are notable: (i) both quantum and classical results show significant control and differ noticeably at the larger  $\hbar_e$  values; (ii) as  $\hbar_e \rightarrow 0$ , the quantum result approaches the classical result. In particular, the  $\phi_{\text{rel}}$  phase dependence of the control dynamics survives in the classical limit, as noted above, where it is identical in quantum and classical mechanics; (iii) as  $\hbar_e \rightarrow 0$ , the quantum result displays the underlying  $\phi_{\text{abs}}$  dependence associated with the regular (second row in Fig. 1) or chaotic (third row) classical behavior.

Thus far, we have considered the general character of the control as  $\phi_{\text{abs}}$  and  $\phi_{\text{rel}}$  are varied. We now focus on the *magnitude* of the control. A quantitative assessment of the degree of control is afforded by the measure

$$R_{(p)} = \max\{\langle P_\theta \rangle\} - \min\{\langle P_\theta \rangle\}, \quad (18)$$

where  $\max\{\langle P_\theta \rangle\}$  and  $\min\{\langle P_\theta \rangle\}$  are the maximum and minimum of the final average momentum across the full space of  $\phi_{\text{abs}}$  and  $\phi_{\text{rel}}$  with  $\hbar_e$  held fixed. Figure 2(a) plots  $R_{(p)}$  over the range of  $\hbar_e=0.001-0.1$  using the uniform initial condition. The horizontal dashed line denotes the classical value of  $R_{(p)}$ , (where the  $R_{(p)}$  uses the classical  $P_{\theta,\text{avg}}$  instead of  $\langle P_\theta \rangle$ ) again for the uniform initial state. Across this range of  $\hbar_e$ , the quantum control ratio varies but is, roughly speaking, always of the same order of magnitude as the classical result or as the  $\hbar_e \rightarrow 0$  limit. Figure 2(b) shows the  $\hbar$  dependence of  $R_{(p)}$  for the chaotic and the regular initial states. One can see that the regular initial state approaches the  $\hbar_e \rightarrow 0$  limit much faster than the chaotic initial state. Essentially, all of the fluctuations seen in Fig. 2(a) as  $\hbar_e \rightarrow 0$  then arise from the chaotic portions of the uniform initial state.

How does the control behave in the large  $\hbar_e$  limit? Figure 2(c) plots  $R_{(p)}$  over a range of  $\hbar_e$  from 0 to 5 for the uniform initial state. The localized regular and chaotic states were not considered since they carry nonzero momentum  $\Delta P_\theta \sim \hbar_e / \Delta\theta$ . There are two main differences between the large  $\hbar_e$  and small  $\hbar_e$  limits. First, the *presence* of control in the large  $\hbar_e$  limit is now strongly dependent on the value of  $\hbar_e$ .

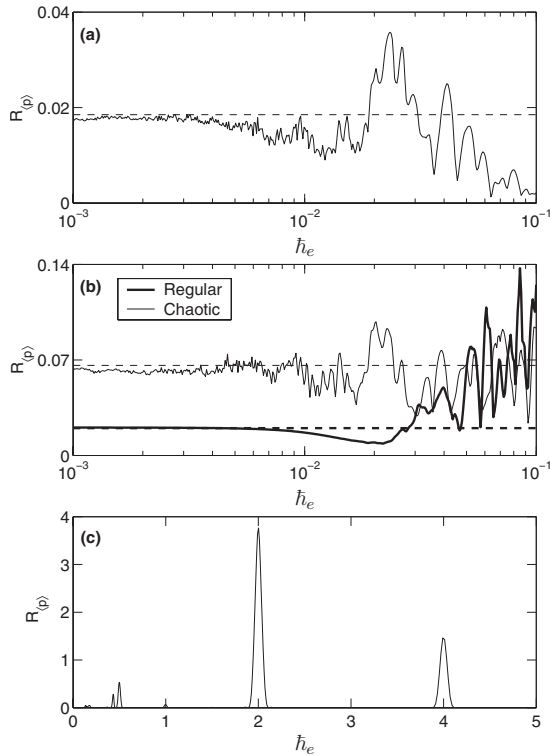


FIG. 2. Magnitude of the control ratio  $R_{(p)}$  (see text for definition) for (a) the uniform initial state for  $\hbar_e \rightarrow 0$ , (b) the chaotic and regular initial states for  $\hbar_e \rightarrow 0$ , and (c) the uniform initial state in the large  $\hbar_e$  regime. The dashed lines in (a) and (b) denote the corresponding classical values of  $R_{(p)}$ .

This is because in the regime of large  $\hbar_e$  the spacing between two adjacent momentum states coupled by the field is large (on the order of  $\hbar_e$ ), and, thus, the allowed transitions depend strongly on the relationship between  $\hbar_e$  and the driving frequencies. Second, when control is present, the magnitude of the control is about two orders of magnitude larger than in the  $\hbar_e \rightarrow 0$  limit. This happens because in the large  $\hbar_e$  limit, the momentum transfer happens in a highly resonant manner between very few states, contrary to the  $\hbar_e \rightarrow 0$  limit where many momentum states are coupled and populated.

#### D. Decoherence in the $\hbar_e \rightarrow 0$ limit

Not all properties of the quantum scenario match the classical scenario perfectly in the  $\hbar_e \rightarrow 0$  limit. For example, in the small  $\hbar_e$  limit (e.g., at  $\hbar_e = 0.0001$ ), the final quantum momentum distribution  $\mathcal{D}_q(P_\theta) = |\Psi(P_\theta)|^2$  [Fig. 3(b)] shows highly oscillatory behavior that is not seen classically [Fig. 3(a)]. These oscillations, arising from quantum interference effects, are superimposed onto the underlying classical distribution and have little or no influence on the average control dynamics. Adding weak decoherence via spontaneous emission (1 momentum jump per cycle of the driving field and of magnitude  $\delta P_\theta = \hbar_e$ ) completely suppresses the oscillations [Fig. 3(d)] and gives the classical distribution, which itself remains unchanged by the addition of the decoherence [Fig. 3(c)]. Similar results were obtained with alternate types of decoherence such as spatial jitter, random amplitude fluctuations,

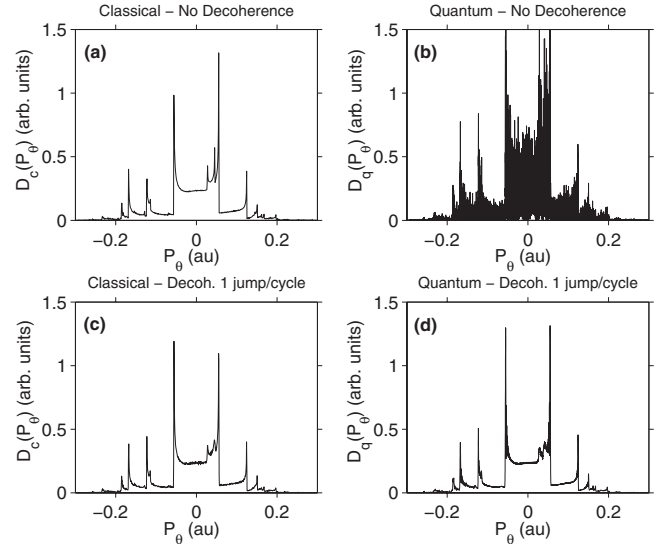


FIG. 3. Classical and quantum momentum distribution (where  $\hbar_e = 10^{-4}$ ) with (panels c and d) and without (panels a and b) decoherence.

or introducing a small initial temperature. Analogous observations of rapid quantum interferences destroyed by small decoherence were made by Ballentine *et al.* in a recent study of the quantum-to-classical transition of Hyperion, a moon of Saturn [20].

Since this small amount of decoherence destroys the quantum interference features and leads to the classical distributions and since phase control is nonetheless present in the classical dynamics, small amounts of decoherence in this scenario remove a fundamentally quantum feature (oscillations in the momentum distribution) but is not detrimental, in the small  $\hbar_e$  limit, to the utility of the coherent control scheme. This contrasts with the usual view that decoherence necessarily jeopardizes coherent control because it mutes quantum interference effects.

#### E. Decoherence in the “large” $\hbar_e$ regime

Can the presence of decoherence accelerate the emergence of quantum-classical correspondence when  $\hbar_e$  is not close to zero? Figure 4 shows the quantum control plots for  $\hbar_e = 0.01$  and the classical control plots for increasing strength of the decoherence. The top plots correspond to no decoherence, the middle plots are for 10% chance of a momentum jump per lattice shaking oscillation, and the bottom plots are for a 20% chance of a momentum jump per lattice shaking oscillation. The magnitude of the momentum jump was set to the value of  $\hbar_e$  used, i.e.,  $\delta P_\theta = 0.01$ . For no decoherence (top row, Fig. 4), the quantum plots have not yet reached the classical behavior for this value of  $\hbar_e$ . As decoherence is increased, the quantum and classical control plots are both modified. However, before quantitative agreement is achieved (an agreement which has not yet set in for the results of Fig. 4), the degree of decoherence would have to be increased to the point where the underlying classical dynamics is modified strongly. This is in contrast with the results of Fig. 3, where the quantum dynamics begins to resemble the

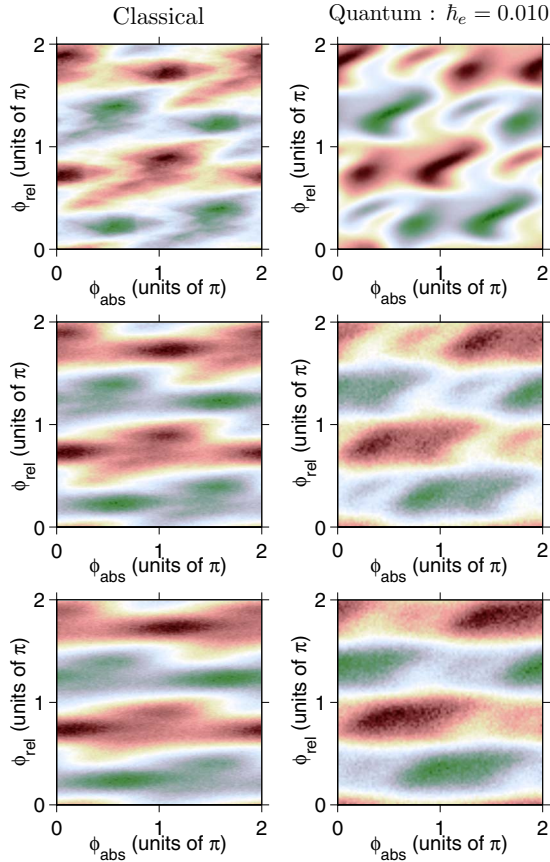


FIG. 4. (Color online) Classical and quantum ( $\hbar_e=0.010$ ) control results for (top) no decoherence, (middle) 10% chance of a momentum jump per cycle, and (bottom) 20% chance of a momentum jump per cycle.

classical dynamics *before* the classical dynamics is modified by the decoherence.

This type of decoherence behavior away from the  $\hbar_e \rightarrow 0$  limit, in which the decoherence must be strong enough to modify the classical dynamics before any hope of quantum-classical correspondence emerges, has been previously reported by one of the present authors in the context of reactive scattering studies [23] in the presence of decoherence and can also be inferred from studies of quantum-classical correspondence under continuous weak measurements [21,22]. In the latter case, the weak measurements, which are affected through weak coupling to external degrees of freedom, can be interpreted as a source of decoherence once one averages over many realization of the weak measurement process.

In the  $\hbar_e < 1$  regime, the effects of small decoherence are fairly general, and as in the previous section, the conclusions reached here are independent of the type of noise used to induce decoherence. However, in the  $\hbar_e > 1$  regime, preliminary computations (not shown) show that this is no longer the case and that effects of decoherence depend strongly on the type of decoherence introduced. The reason for these complications is that, in the present shaken lattice scenario, the classical system has no resonances, whereas the dynamics of the quantum when  $\hbar_e > 1$  is dominated by the resonance behavior [recall Fig. 2(c)]. In such a case, the quantum and classical systems behave qualitatively differently. A thor-

ough study of decoherence in the  $\hbar_e > 1$  regime departs from the central focus of this paper, quantum-classical transition of a coherent control scenario, since the two systems are now qualitatively different and no general quantum-classical correspondence via decoherence when  $\hbar_e > 1$  is expected. For these reasons, we leave the investigation of decoherence in the  $\hbar_e > 1$  regime for a separate study. For recent related studies on quantum-classical correspondence and decoherence in the quantum resonance case, see Refs. [24,25].

#### IV. SUMMARY AND COMMENTS

In summary, we have shown the quantum-to-classical transition of control in the  $\omega$  vs  $2\omega$  coherent control scenario in an experimentally accessible optical lattice experiment, either isolated or in the presence of tunable amounts of decoherence. Clear evidence of the approach of the quantum control to the classical limit is evident, including the manifestation of chaotic vs integrable classical dynamics. Decoherence associated with spontaneous emission is seen to destroy high-frequency oscillations in the momentum distribution, but not to affect the control in the small  $\hbar_e$  limit. Significant effects on the quantum control due to decoherence were only found to arise in the case where the decoherence is so strong as to have a profound effect on the classical dynamics, as well as the quantum dynamics.

The results are of fundamental significance to the general area of coherent control and motivate additional work. First, the results emphasize the fact that quantum-based coherent control scenarios can persist in the classical limit, albeit that the numerical values of the control can be vastly different in the quantum and classical regimes. This correspondence, as noted here and elsewhere [6], arises because the quantum interference terms are driven by the external laser fields. Our expectation is that any quantum control scenario that can be cast as a nonlinear response problem falls into this class. What remains to be explored are (a) the circumstances under which the quantum results are well approximated by the classical dynamics [26] and (b) the range of scenarios that are fully quantum—i.e., that rely upon fully quantum effects, such as entanglement, and hence do not survive classically. Second, the decoherence results shown here are relevant to the optical lattice setup, where decoherence results from spontaneous emission. Other types of open system interactions, in accord with the decoherence literature, can be expected to induce decoherence to other preferred bases [18,19]. This being the case, different coherent control scenarios that occur in alternate environments may well behave differently. For example, and of particular interest to chemical physics, are systems undergoing decoherence in condensed phase environments. Studies on decoherence associated with random collisions characteristic of such environments suggest that such decoherence may be particularly destructive to coherent control scenarios [7]. Further studies of these effects are underway.

#### ACKNOWLEDGMENT

This work was supported by NSERC Canada.

- [1] M. Shapiro and P. Brumer, *Principles of the Quantum Control of Molecular Processes* (Wiley, New York, 2003).
- [2] S. A. Rice and M. Zhao, *Optical Control of Molecular Dynamics* (Wiley, New York, 2000).
- [3] S. Flach, O. Yevtushenko, and Y. Zolotaryuk, Phys. Rev. Lett. **84**, 2358 (2000).
- [4] V. Constantoudis and C. A. Nicolaides, J. Chem. Phys. **122**, 084118 (2005).
- [5] I. Franco and P. Brumer, Phys. Rev. Lett. **97**, 040402 (2006); J. Phys. B **41**, 074003 (2008).
- [6] I. Franco, M. Spanner, and P. Brumer (unpublished).
- [7] I. Franco, Ph.D. dissertation, University of Toronto, 2007.
- [8] G. Kurizki, M. Shapiro, and P. Brumer, Phys. Rev. B **39**, 3435 (1989).
- [9] E. Dupont, P. B. Corkum, H. C. Liu, M. Buchanan, and Z. R. Wasilewski, Phys. Rev. Lett. **74**, 3596 (1995).
- [10] R. Atanasov, A. Hache, J. L. P. Hughes, H. M. van Driel, and J. E. Sipe, Phys. Rev. Lett. **76**, 1703 (1996).
- [11] M. Schiavoni, L. Sanchez-Palencia, F. Renzoni, and G. Grynberg, Phys. Rev. Lett. **90**, 094101 (2003).
- [12] P. H. Jones, M. Goonasekera, and F. Renzoni, Phys. Rev. Lett. **93**, 073904 (2004); R. Gommers, S. Bergamini, and F. Renzoni, *ibid.* **95**, 073003 (2005); R. Gommers, S. Denisov, and F. Renzoni, *ibid.* **96**, 240604 (2006), and references therein.
- [13] A. Zenesini, H. Lignier, D. Ciampini, O. Morsch, and E. Arimondo, Phys. Rev. Lett. **102**, 100403 (2009).
- [14] S. Denisov, L. Morales-Molina, and S. Flach, EPL **79**, 10007 (2007).
- [15] D. A. Steck, W. H. Oskay, and M. G. Raizen, Science **293**, 274 (2001); Phys. Rev. Lett. **88**, 120406 (2002).
- [16] G. Ball, K. Vant, and N. Christensen, Phys. Rev. E **61**, 1299 (2000).
- [17] R. Loudon, *The Quantum Theory of Light*, 2nd ed. (Oxford University Press, New York, 1983).
- [18] E. Joos, H. D. Zehm, C. Kiefer, D. Giulini, J. Kupsch, and I.-O. Stamatescu, *Decoherence and the Appearance of a Classical World in Quantum Theory*, 2nd ed. (Springer-Verlag, Berlin, 2003).
- [19] M. Schlosshauer, *Decoherence and the Quantum-To-Classical Transition* (Springer-Verlag, Berlin, 2007).
- [20] N. Wiebe and L. E. Ballentine, Phys. Rev. A **72**, 022109 (2005).
- [21] S. Ghose, P. Alsing, I. Deutsch, T. Bhattacharya, S. Habib, and K. Jacobs, Phys. Rev. A **67**, 052102 (2003).
- [22] S. Ghose, P. Alsing, I. Deutsch, T. Bhattacharya, and S. Habib, Phys. Rev. A **69**, 052116 (2004).
- [23] H. Han and P. Brumer, J. Chem. Phys. **122**, 144316 (2005).
- [24] E. F. de Lima and M. A. M. de Aguiar, Phys. Rev. A **77**, 033406 (2008).
- [25] A. Romanelli, e-print arXiv:0905.0703.
- [26] The fact that classical and quantum nonlinear response can be vastly different has been emphasized in M. Kryvohuz and J. S. Cao, Phys. Rev. Lett. **96**, 030403 (2006).